Biophysical Chemistry 146 (2010) 85–91

Contents lists available at ScienceDirect

Biophysical Chemistry

journal homepage: http://www.elsevier.com/locate/biophyschem

Adsorption of pepsin in octadecylamine matrix at air–water interface

Tapanendu Kamilya [a,b], Prabir Pal [a], G.B. Talapatra [a,*]

[a] Department of Spectroscopy, Indian Association for the Cultivation of Science, Jadavpur, Kolkata-700 032, India
[b] Department of Physics, Narajole Raj College, Paschim Medinipur-721 211, India

ARTICLE INFO

Article history:
Received 22 September 2009
Received in revised form 16 October 2009
Accepted 27 October 2009
Available online 3 November 2009

Keywords:
Langmuir–Blodgett Film
Pepsin
Octadecylamine
Lipid–protein interaction
FE-SEM
FTIR

ABSTRACT

The incorporation/entrapment of water-soluble surface-active enzyme, pepsin (PEP) within an insoluble cationic octadecylamine (ODA) monolayer is studied by Langmuir–Blodgett technique. The observation suggests that the incorporation of PEP is less preferable at compressed region (~30 mN/m). The electrostatic interaction plays a significant role for the greater incorporation of PEP in cationic ODA monolayer. The surface pressure–area isotherms along with FE-SEM analysis indicates the squeezing out of PEP from the monolayer at higher surface pressure. This will assist to select the optimum surface pressure to obtain a good quality and well-ordered Langmuir monolayer. FTIR study of amide bands together with FE-SEM imaging of ODA–PEP mixed film indicates that ODA perturbs the PEP by the increment of β-structure resulting into larger unfolding, intra, and intermolecular aggregates.

1. Introduction

The encapsulation of protein/enzyme in different lipid matrices is a subject that has received considerable attention in recent years to protect the protein/enzyme against microbial degradation, hydrolysis, and auto proteolysis as well as for prospective biotechnological devices fabrication along with biomedical applications [1–8]. Numerous methods, such as sol–gel process, self-assembly (SA), Langmuir Blodgett (LB) techniques etc. [9–15] are proposed for immobilizing proteins in lipid matrices. Among these, the Langmuir and/or Gibbs monolayer studies and subsequent monolayer transfer to solid substrate by LB techniques are the most versatile and convenient techniques to study the protein–lipid interaction at air/water interface for entrapment of protein/enzyme in lipid matrices as well as for designing ultra thin artificial films with biological functions [16].

Depending on the isoelectric point (pI) of the protein/enzyme, cationic amphiphilic reagent (e.g. octadecylamine) has been used to immobilize proteins in many investigations [1,17–20]. However, the conformational regulation and orientation of protein/enzyme in octadecylamine (ODA) matrix is not well established.

In the present study, our intention is to investigate the interaction of a proteolytic enzyme, pepsin (PEP) which exists in the gastric juice of all mammals [1] with octadecylamine at air/water interface. Aim lies also to study the formation of ODA–PEP mixed LB film along with the measurement of structural reorganization of PEP. By combined use of LB deposition and high-resolution FE-SEM techniques, this study focuses on the structural aspects of PEP on ODA monolayer. The surface pressure (π) versus time (t) curves in addition to the surface pressure (π) versus area (A) isotherms were studied to understand the physical aspect of PEP–ODA interaction as well as the incorporation of PEP within the ODA surface. FTIR spectroscopy of amide bands of PEP were utilized to inspect the extent of the conformational transitions of PEP in immobilized PEP–ODA film.

2. Experimental

PEP and ODA were purchased from Lobachemie and Aldrich Chemical Co., respectively. These chemicals were used as received without further purification. The spectral grade chloroform (SRL, India) was used as solvent to prepare solution of ODA with desired concentrations. A Teflon-bar-barrier type LB trough (model 2000C, Apex Instruments Co. India) was used for the preparation, characterization and deposition of film. The trough width and length are 200 mm and 450 mm respectively. The subphase volume is about 1.2 L. The subphase used was triple distilled water, deionized with a Milli-Q water purification system from Millipore. The pH and the resistivity of the freshly prepared distilled water were 6.8 and 18.2 MΩ cm, respectively. All the experiments were performed at temperature 26 ± 1 °C unless otherwise mentioned.

To study the adsorption behavior of PEP at bare air/water interface, PEP was injected into the water subphase from the previously prepared aqueous stock solution to attain the required final concentration (0.1 mg/mL) in subphase of LB trough.

To study the adsorption kinetics of PEP in ODA monolayer at constant area, the pure ODA monolayer was pre-compressed to requisite surface pressure and then the aqueous solution of PEP was injected into the subphase to attain the required final concentration. The details of

* Corresponding author. Tel.: +91 33 24734971; fax: +91 33 24732805.
E-mail address: spgbt@iacs.res.in (G.B. Talapatra).

0301-4622/$ – see front matter © 2009 Elsevier B.V. All rights reserved.
doi:10.1016/j.bpc.2009.10.008

experimental processes were similar with our previous experiment described elsewhere [10,17].

For the preparation of pure PEP film, a known amount of aqueous solution of PEP of concentration 1 mg/mL was spread on the water subphase by a microsyringe. A similar technique was used for the preparation of ODA monolayer where chloroform solution of ODA (1 mM) was spread on the water subphase by a micro syringe. For the surface pressure–area isotherm measurement of PEP–ODA system, first we mixed the PEP with subphase with concentration of PEP ranging over 0.0001, 0.0005, and 0.001 mg/mL. The ODA solution was then spread on this PEP containing subphase. In all above-mentioned cases, the films were compressed to the required surface pressures with a compression speed of 1 $Å^2$/(molecule min), after a delay of 20 min from spreading. It is worth to mention that during this waiting time, some PEP molecule will make a complex with ODA molecule and some free PEP molecules may occupy holes of free air water interface. Delay of 20 min is found optimum for stable monolayer configuration of PEP, PEP–ODA complex.

Finally, after 2 h of stabilization, all the films were transferred very carefully with a speed of 5 mm/min onto thoroughly cleaned hydrophilic glass cover slips and silicon wafers, which were previously immersed in the subphase. The detail cleaning procedure was reported in our earlier literature [12].

The surface morphology of all films was studied by high-resolution field emission scanning electron microscope (FE-SEM, model no JEOL JSM-6700 F).

FTIR spectra of PEP in all films on silicon wafer substrate were recorded at room temperature on Magna-IR (Model No 750 spectrometer, series II), Nicolet, USA. In all the cases, the data were averaged over 100 scans. The resolution of the instrument is 4 cm^{-1}.

3. Result and discussion

3.1. Kinetics of PEP incorporation/association within ODA monolayer

In our earlier work [21], we have studied in detail the interfacial surface activity of PEP at air/water interface by monitoring the time (t) dependent surface pressure (π) at various concentrations of PEP (C_{PEP}). The C_{PEP} dependent π–t curves showed that there were initial lag times (τ_{lag}) where π values remained near zero. This initial lag phase is the diffusion-limited regime, a significant characteristic of protein adsorption process, where the interface is lacking sufficient quantity of PEP for noticeable change in π. This lag time (t_{lag}) is the time required for attaining the minimum monolayer coverage for an effective and measurable surface pressure [21,22]. After t_{lag}, there is faster increase of π followed by a slower increase. In the first step, the diffusion of molecule to the subsurface just below the interface is effective, whereas in the second step the adsorption of protein/enzyme molecules at the air/water interface is effective. In the second step, the adsorbed protein molecules rearrange among themselves resulting in partial unfolding of adsorbed segment [21–23]. Earlier studies [21] also showed that the increase of C_{PEP} decreases τ_{lag} and makes the diffusion rate faster, as a result more pepsin molecules comes to surface very quickly and less time is required to attain saturation. We have found out the optimum/critical concentration of pepsin to fill up the surface after which no further penetration takes place. The critical pepsin concentration observed in our experiment was 0.1 mg/ml.

The curve A of panel X in Fig. 1 (taken from our earlier study [21]) shows the increase of π for the PEP solution of final concentration (C_{PEP}) of 0.1 mg/mL. Here PEP was injected inside the water subphase. To visualize clearly the panel Y of Fig. 1 displays the same up to 500 s. The π–t curve shows a lag phase up to $t = 160$ s where the π values remains near zero.

To study the incorporation kinetics of PEP within the ODA monolayer at the air/water interface, the monolayer of ODA was compressed to a particular surface pressure (π_{pc}), in the pure water subphase and then an amount of PEP solution was injected into the water subphase to obtain the required final concentration. Curves B–E of panel X in Fig. 1 represent the time dependent changes in surface pressure of the ODA monolayer pre-compressed at various π_{pc}, when a fixed amount (0.1 mg/mL final concentration) of PEP was injected beneath the ODA monolayer in the water subphase.

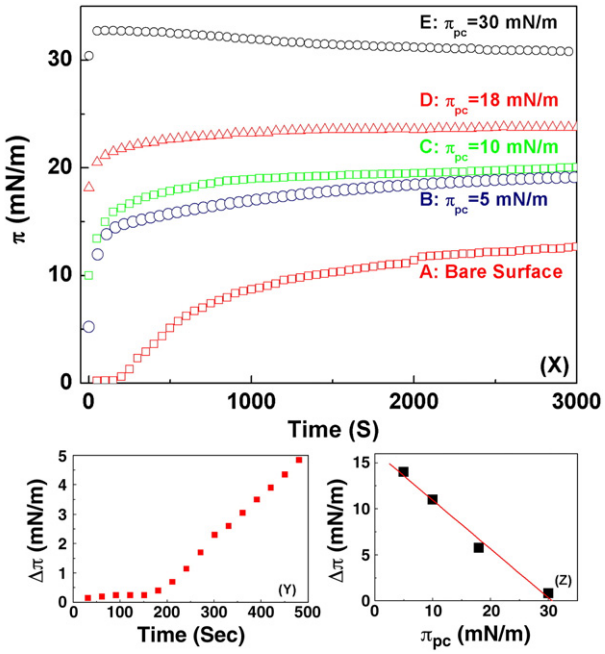

Fig. 1. Panel X represents the surface pressure (π)–time (t) plot. Curve A: Adsorption of PEP at bare air/water interface. The curves B–E represent the π–t plot at different pre-compressed π_{pc} of ODA monolayer when PEP is injected beneath the ODA monolayer. Corresponding π_{pc} for B, C, D, and E curves are 5, 10, 18, and 30 mN/m surface pressure respectively. In each case, the protein concentration in the subphase is maintained at 0.1 mg/ml. Panel Y represents the plot of change of surface pressure ($\Delta\pi$) with time for the Curve A of panel X up to 500 s. Panel Z represents the plot of $\Delta\pi$ at different pre-compressed surface pressure (π_{pc}). The line is the linear fit.

The result shows that the addition of ODA at the air/water interface alters the shape of the curve. An immediate increment of π is observed and the equilibrium is attained within same duration, implies that the PEP molecules interact and incorporate with the ODA monolayer. The inset of Fig. 2 shows the structures of ODA and PEP

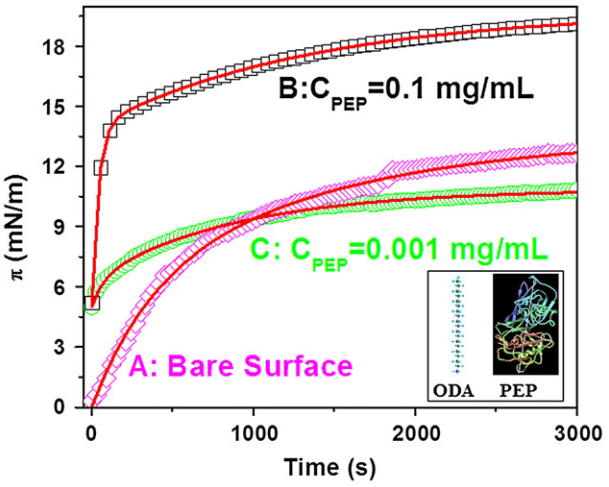

Fig. 2. Surface pressure (π)–time (t) plot. Curve A: Adsorption of PEP at bare air/water interface. Here the lag time part is rejected. Curves B and C represent the growth of PEP below ODA monolayer pre-compressed at 5 mN/m with $C_{PEP} = 0.1$ and 0.001 mg/mL, respectively. The solid lines are the fitted curves using the Eq. (1). Inset shows the structures of ODA and PEP.

Table 1
Fitting parameters using Eq. (1) of adsorption kinetics of PEP with different PEP concentration in water subphase in presence and absence of ODA.[a]

	C_{PEP}. (mg/mL)	A_1	t_1 (s.)	A_2	t_2 (s.)	R^2
No ODA	0.1	5.62 ± 0.01	352.14 ± 4.71	8.01 ± 0.08	1401.06 ± 18.99	0.998
ODA at 5 mN/m	0.1	9.41 ± 0.04	37.70 ± 0.83	5.84 ± 0.03	1350.30 ± 3.49	0.999
ODA at 5 mN/m	0.001	1.35 ± 0.01	69.83 ± 1.12	4.50 ± 0.01	893.86 ± 3.44	0.999

[a] A_1 and A_2 are the relative amplitudes and t_1 and t_2 are corresponding time constants of two mechanisms involving in association process. (R^2) is the residual square correlation coefficient.

monomer collected from Protein Data Bank (PDP 5 PEP) PEP molecule is amphiphilic in nature. Helical parts are generally hydrophobic in nature whereas β-sheets and turns are hydrophilic in nature. In aqueous solution protein folds itself to keep hydrophobic part away from water. At pH 6.8, the ODA monolayer is positively charged (pK_B of ODA = 10.5) [19], whereas the PEP molecules are negatively charged (pI of PEP = 1.0) [24], thus due to attractive electrostatic interaction a rapid diffusion of PEP into ODA matrix is observed. Moreover, the hydrophobic interaction together with the electrostatic may be responsible for higher accumulation of the protein at the air/water interface in presence of ODA. The similar observation of increase of surface activity of ovalbumin in presence of ODA was reported in our earlier literature in detail [17].

It is found that $\Delta\pi = \pi_t - \pi_{pc}$ (π_t represents the surface pressure at time t) at $t = 3000$ s decreases with the increase of π_{pc} as shown in the panel Z of Fig. 1. At $\pi_{pc} = 30$ mN/m, a very small amount of PEP uptake occurs. At higher π_{pc}, due to small amount of PEP penetration, the change in surface pressure becomes less significant. This plot of $\Delta\pi$ versus π_{pc} gives the value of the critical surface pressure (π_c) at ~31.0 mN/m. π_c is the surface pressure at which the protein cannot produce any further increase of surface pressure. Moreover, the increment of surface pressure at the expanded region is more than that of at the condensed region. These results clearly demonstrate that the protein penetration behavior is different in the above-mentioned two cases. The protein association or incorporation facilitates in the expanded region. The slower adsorption kinetics of PEP at the interface in presence of condensed ODA film compared to expanded film could be due to the difference in permeability of the respective ODA monolayers. Only negligible amount of PEP penetrates in condensed ODA film and thus the surface pressure remains unaltered. A slow protein attachment process is also competing here. Similar observations were found for ovalbumin in DPPC, ODA and SA [10,17,20] as well as puroindoline in DPPC and in DPPG monolayer [25].

For analyzing the kinetics of PEP association, the adsorption curves are fitted to double exponential association mechanism using following equation [17,20,26].

$$\pi_t = \pi_0 + A_1\left[1 - \exp\left(-t/t_1\right)\right] + A_2\left[1 - \exp\left(-t/t_2\right)\right] \quad (1)$$

π_t and π_0 in Eq. (1) are the surface pressures at time t and zero respectively. Constants A_1, and A_2 are the relative amplitudes and t_1 and t_2 are corresponding time constants of two mechanisms (diffusion with adsorption and rearrangement with unfolding) involved in the adsorption process [10]. A relative contribution of both mechanisms among the monolayer containing different amounts of protein may be obtained from these parameters A_1, and A_2. A non-linear least square fitting based on Levenberg–Marquardt algorithm of Microcal Origin 7.5 was used for curve fitting.

Curve A in Fig. 2 shows the growth curve at bare air/water interface after discarding the initial part belongs to the lag time and rescaled the adsorption curves, where the zero time has been adjusted when the surface pressure starts to increase [21]. Curves B and C in Fig. 2 represent the growth of PEP below ODA monolayer pre-compressed at 5 mN/m with $C_{PEP} = 0.1$, 0.001 mg/mL, respectively. The growth curves show reasonably good fits with residual square correlation coefficient (R^2) ≥ 0.99. The parameters resulting from the fits are summarized in Table 1.

At $C_{PEP} = 0.1$ mg/mL, the value of t_1 decreases and A_1 increases in presence of ODA compared to bare air/water interface implies that diffusion of PEP is faster in presence of ODA and uptake of more PEP occurs. The value of t_2 is almost similar in both ODA–PEP system and pure PEP. Increment of value of A_1 and decrement in t_1 with the increment of C_{PEP} at the same pre-compressed ODA monolayer, indicates that diffusion of PEP increases with concentration of PEP. The above results indicate that the strong electrostatic interaction between ODA and PEP.

3.2. π–A isotherm study

We have discussed in detail the behavior of the π–A isotherm of PEP monolayer at air/water interface [21]. Fig. 3(A) represents the π–A isotherm of Langmuir monolayer of ODA on the water subphase, exhibits a condensed monolayer on the subphase of pure water at pH 6.8. Area/molecule starts to increase at ~0.22 nm^2/ODA similar to that reported in the literature [19]. The curves B, C and D in Fig. 3 trace the π–A isotherms of mixed Langmuir monolayer of ODA–PEP with $C_{PEP} = 0.0001$, 0.0005 and 0.001 mg/mL in the water subphase respectively. In our earlier literature [21], we discussed in detail about the π–A isotherm of monolayer of PEP on the pure aqueous subphase. We have included here the same (Fig. 3(E)), to compare it with other isotherms of PEP–ODA mixed monolayer. The π–A isotherms of PEP–ODA mixed monolayers show sigmoidal shape [17,27]. With increasing concentration of PEP in the water subphase, the area/molecule of ODA increases, indicates the incorporation of PEP within the ODA monolayer. All the mixed isotherms of PEP–ODA cross

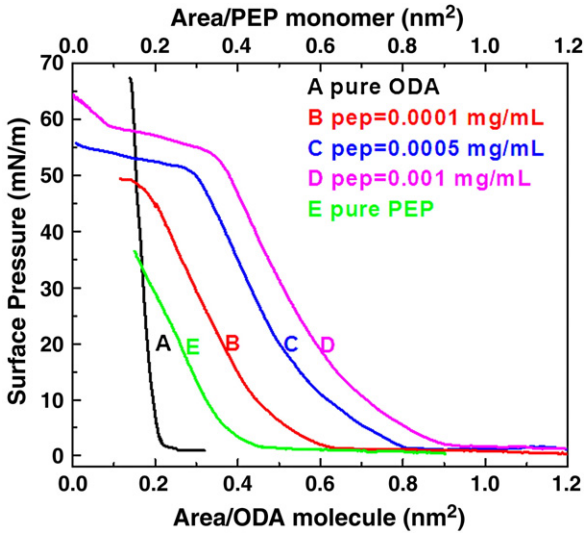

Fig. 3. Plot of surface pressure (π)–area (A) isotherm at room temperature (26 °C). Curve A: Pure ODA at air/water interface. The curves B–D represent the isotherms of ODA–PEP mixed monolayer with $C_{PEP} = 0.0001$, 0.0005 and 0.001 mg/mL, respectively. Curve E: Pure PEP at air/water interface. The bottom axis is for curves A, B, C, and D and the top axis is for curve E. In ODA–PEP mixture, the area/molecule is measured with respect to ODA only.

the pure ODA isotherm at higher surface pressures. A complete expulsion or successive squeezing out of Pepsin can interpret this observation. Other authors have come to the same conclusions with similar observations [19,27–29] for different proteins and lipids. With further compression, the area/molecule for the mixed monolayer is found to be less than the pure ODA, as C_{PEP} increases. This phenomenon is more prominent in the case of higher protein concentration. At high surface pressure, in the process of squeezing out, the PEP molecules those are already bounded with the ODA may also drag out ODA molecules from the air/water interface. Others [19,30] interpreted similar observation in the same way. As mentioned earlier, that at subphase of pH 6.8 a strong electrostatic interaction between the ODA and the PEP is expected, so at high surface pressure, the PEP molecules may drag the ODA molecules with them [31]. This observation indicates that the interaction between PEP and ODA is very strong.

The two-dimensional surface compressibility analysis of the Langmuir monolayer is performed to understand the presence as well as details of phase transition [32–36]. The compressibility coefficient (β) is calculated using the following equation [32].

$$\beta = -\left({}^{1}/_{A}\right).\left({}^{\delta A}/_{\delta \pi}\right)_{T} \quad (2)$$

Here, π and A represent the surface pressure and area/molecule of the monolayer respectively at constant temperature (T). Any phase transition could be represented by the β–π curve whose peaks indicate the maximum compressibility (β_{max}) of the monolayer. β_{max} represents the greatest intermolecular cooperativeness. The asymmetry of the peak indicates that phase transition may consist of several steps [32].

The Fig. 4 shows the β–π curves for ODA, ODA–PEP and PEP isotherms. The Fig. 4(A) represents the β–π curve for pure ODA. We have not found any phase transition region in the π–A isotherm for pure ODA. Yin et al. [34] reported similar observation. The β–π curves of the ODA–PEP mixed monolayers with different PEP concentrations are illustrated in Fig. 4(B to D). The β–π curve of the pure PEP shows a broad peak at π ~32 mN/m represented in Fig. 4(E), taken from our earlier literature [21] where more detail description was presented. This broad peak for pure PEP arises due to partial squeeze-out of PEP from the monolayer, preceding the full collapse [21]. Whereas, the peak due to squeeze-out of PEP was found at π~35 mN/m for the ODA–PEP mixed monolayers. The change of the width of the peak is the manifestation of the interaction and binding of PEP with ODA. The peak corresponds to the beginning of a progressive expulsion of PEP from the mixed monolayer into the subphase upon compression, observed by FE-SEM image. It will be discussed in the appropriate section. Moreover, from the β–π curves, it is evident that the maximum compressibility, β_{max} of this transition is dependent on the PEP concentration. The β_{max} at this transition region of the ODA–PEP complex layer with different amounts of PEP increases, with the increasing PEP concentration (C_{PEP}) in the subphase (inset of Fig. 4). Therefore, it is necessary to transfer a better and smooth protein–lipid mixed film below the transition point (π at β_{max}) of the PEP monolayer to avoid the squeezing out of PEP. The compressibility peaks are quite symmetric in all the cases. Therefore, one step transition process is involved in both cases. Absence of any large shifting of peaks (β_{max}) in ODA–PEP monolayer predicts no such hydrophobic mismatch is involved in the process of PEP incorporation. We believe that the hydrophobic mismatch is not operating in case of ODA–PEP due to strong electrostatic interaction between ODA and PEP.

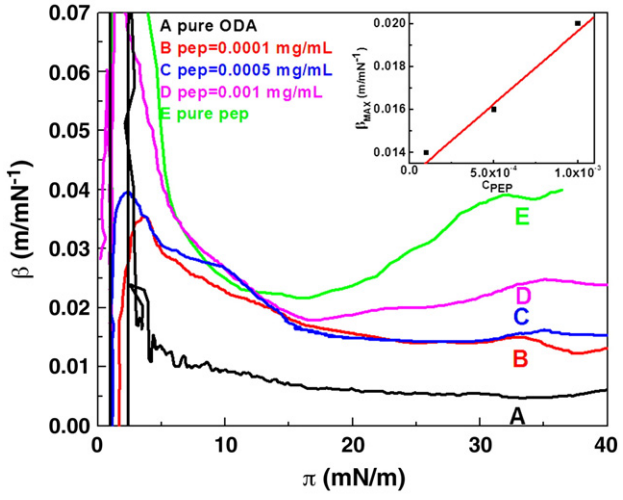

Fig. 4. Plot of compressibility (β)–surface pressure (π) at room temperature (26 °C). Curve A: Pure ODA at air/water interface. The curves B–D represent the isotherms of ODA–PEP mixed monolayer with C_{PEP} = 0.0001, 0.0005 and 0.001 mg/mL, respectively. Curve E: Pure PEP at air/water interface. The inset shows β_{max} vs C_{PEP} plot of the PEP–ODA monolayer.

3.3. FTIR study

FTIR spectra of LB film of protein/enzyme are very useful tool to identify the unfolding, denaturation, intra- and intermolecular aggregation of protein/enzyme by monitoring its amide bands within a fixed range [37]. The amide-band of protein mainly comprises of amide-I (~1600 to 1700 cm^{-1}) and amide-II (~1500 to 1600 cm^{-1}). The panels A and B of Fig. 5 represent the FTIR spectra of thin monolayer film of PEP and PEP–ODA lifted from pure water subphase at π = 35 mN/m respectively. Both the spectra consist of two broad peaks arising from amide-I and from amide-II. The vibration band of amide-I is mainly resulted from carbonyl stretching vibrations of the peptide backbone, which depends on the strength of hydrogen bond and the interactions between the amide units, also amide-II is due to the combination of N—H in-plane bending and C—N stretching vibrations of peptide groups [37,38]. We have not compare the amide-II regions of the FTIR spectra of thin film of PEP and PEP–ODA, since both the vibrations of PEP and ODA head group overlap in amide-II region. The vibration band of amide-I is thus sensitive to the peptide secondary structures that span different components, such as α-helix, β-sheets, β-turns, random coil structure, intra and intermolecular aggregates. The determination and the assignment of the spectral components of the amide-I band can then provide information on the secondary structure of protein [37,39]. We have analyzed the amide-I band to find out about the intra- and intermolecular aggregates as well as the formation of β-sheet to study the conformations of PEP. However, the most crucial point is the assignment as well as the deconvolution of the different components of secondary structure in amide-I band. This is generally, done by Gaussian fitting to describe the components [40]. A multiple peak fitting technique with Gaussian profile was employed to fit normalized amide-I band that allows one to identify and determine the peak frequencies of different components [41]. In addition, the percentage area of the corresponding deconvoluted peaks gives the relative amount of conformers. We have tried to make a second derivative of the amide-I band to find both the position and the number of the peaks. It is worth noting that in all the spectra considered in the present work, the maximum number of the components (N), which can be identified in the deconvoluted amide-I band, are 5 for pure PEP film and 6 for PEP–ODA film to have a meaningful fitting. These values are also obtained from second derivative spectrum presented as upper curve in the panels C as well as in D in Fig. 5.

Since the secondary structures are stabilized by hydrogen bonds between amide C O and N—H groups, the position of the components

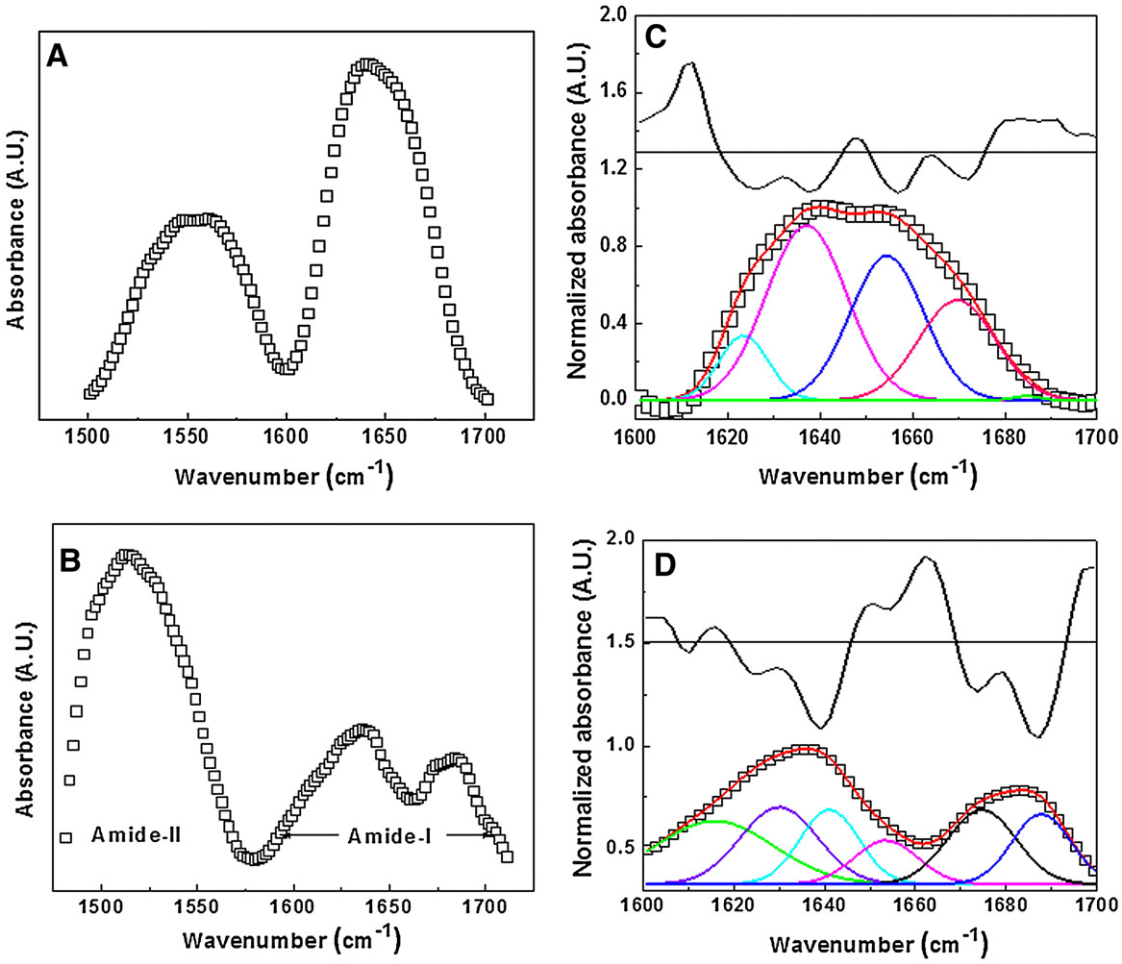

Fig. 5. FTIR spectra of amide-I and amide-II band. Panel A: PEP monolayer film. Panel B: ODA–PEP LB film. Panel C: multi-peak fitting curves of normalized amide-I band of A. The upper curve of panel C represents the double derivative spectrum of C. D: multi-peak fitting curves of normalized amide-I band of B. The upper curve of panel D represents the double derivative spectrum of B.

depends on the patterns and the strength of the hydrogen bonds. Hydrogen bonding causes shifting of the vibration at lower wave number. The β-sheet structures have the strongest hydrogen bonds, exhibit an amide-I maximum at much lower frequency than α-helices [38]. The 1618 cm^{-1} and 1683 cm^{-1} bands are assigned to inter (A_1 component) and intra-molecular aggregates (A_2 component) respectively [37]. In case of aggregates, the hydrogen bonds formed between C O and N—H groups of any polypeptides strands with which they come in contact. The consequence is that many hydrogen bonds are formed between polypeptide chains in neighboring protein molecule, forming an aggregate stabilized by very strong intermolecular hydrogen bonds [38]. The 1666 cm^{-1} component can be ascribed to the vibration modes originated by β-turns in the structures (T-component) [37,38,42–47]. The 1645 cm^{-1} band is assigned to random coil (RC) [48].

The panels C and D of Fig. 5 represent the fitting curves of normalized amide-I peak of LB thin films of PEP and PEP–ODA lifted from pure water subphase and fitting results are reported in Table 2. For all the fittings the square of the correlation coefficient, R^2 is found to be 0.999. The summary of the fitting result is presented in Fig. 6 by bar diagram and in Table 2. The β/α ratio for different films are presented in the inset of Fig. 6.

The Fig. 6 and Table 2 show that the monolayer of PEP lifted from pure water subphase is composed of high amount of β-component (39.42%) and relatively small amount of α-component (29.73 %). Since the β/α ratio (1.325) is greater than unity, some α helix may be converted into β sheet. In addition, large values of A_1 (8.94%) and low value of A_2 (0.35%) indicate that there are mostly larger intermolecular aggregates. The LB thin film of PEP–ODA lifted from pure water subphase is also composed of relatively high amount of A_1 (25.01%), A_2 (13.80%) and β-component (19.90%) and of small amount of α-component (9.34 %). The β/α ratio (2.131) is greater than monolayer film of pure PEP lifted from pure water subphase. Thus, more amount of α helix may convert into β sheet as well as forms intermolecular aggregates in case of mixed ODA–PEP film than pure PEP monolayer. We have also found a large amount of RC structure (14.74%) in case of mixed ODA–PEP film. This component was not found in pure PEP monolayer. Moreover, large value of A_1 (25.01%), A_2 (13.80%) as well

Table 2
Fitting parameters of amide-I band for PEP thin film.[a]

Conformers	Area (%)		Position (cm^{-1})		FWHM (cm^{-1})	
	A	B	A	B	A	B
A_1	8.94	25.01	1623.4	1615.8	10.61	25.99
β	39.42	19.90	1637.0	1630.0	17.43	16.92
RC	–	14.74	–	1641.1	–	12.94
α	29.73	9.34	1654.5	1653.5	15.93	13.98
T	21.56	17.21	1669.6	1674.6	16.64	15.14
A_2	0.35	13.80	1684.7	1687.7	05.94	12.89

[a] A: monolayer film of pure PEP lifted from bare air/water interface, B: ODA–PEP LB film lifted from air/water interface. Area (%) = 100 represents the total area under curve. FWHM is full width at half maximum of a peak.

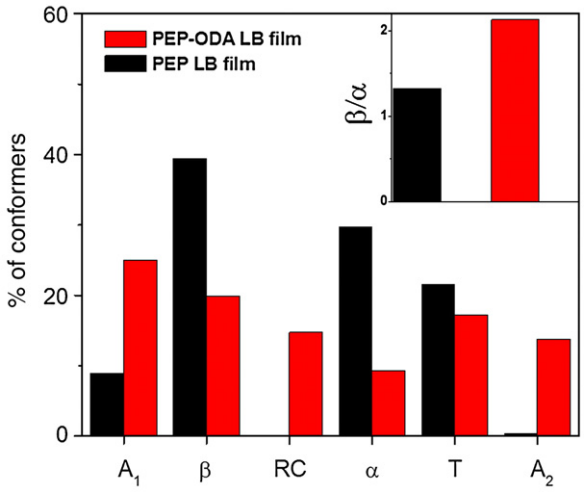

Fig. 6. Bar diagram of the result obtained from Fig. 5C and D.

as high amount of RC structure indicate that there are mostly larger intermolecular aggregates with greater unfolding of PEP occurs in ODA–PEP mixed film.

3.4. Surface morphology of transferred monolayer

The surface morphology of the transferred monolayers was observed by high-resolution FE-SEM. The panels A, B and C in Fig. 7 represent the surface morphology of transferred monolayer of pure ODA, pure PEP, and PEP–ODA, transferred at condensed state (35 mN/m) on a hydrophilic glass substrate, respectively.

In case of pure ODA (panel A), the film is almost compact with the aggregated domains of sizes are around 100 nm. In the condensed region, the growth of the ODA domains is reported in the literature [17,49].

The panel B shows that surface morphology of the PEP film transferred at $\pi = 35$ mN/m. It consists of two layers. The upper layer consists of larger clusters (20–30 nm) peeping out from the surface. The PEP molecules squeezed out from the air/water interface leads to cluster formation due to greater unfolding of PEP molecules those were in completely in the air phase [21]. Therefore, FE-SEM image supports the observations and the arguments of the π–A isotherm. Although the origin of squeeze-out of the protein is not very clear to us, but the desorption of hydrophobic moieties of PEP from the air/water interface due to high surface pressure may be the cause of squeezing out of protein.

Panel C in Fig. 7 shows the surface morphology of the ODA–PEP monolayer at condensed region (35 mN/m) in micrometer scale

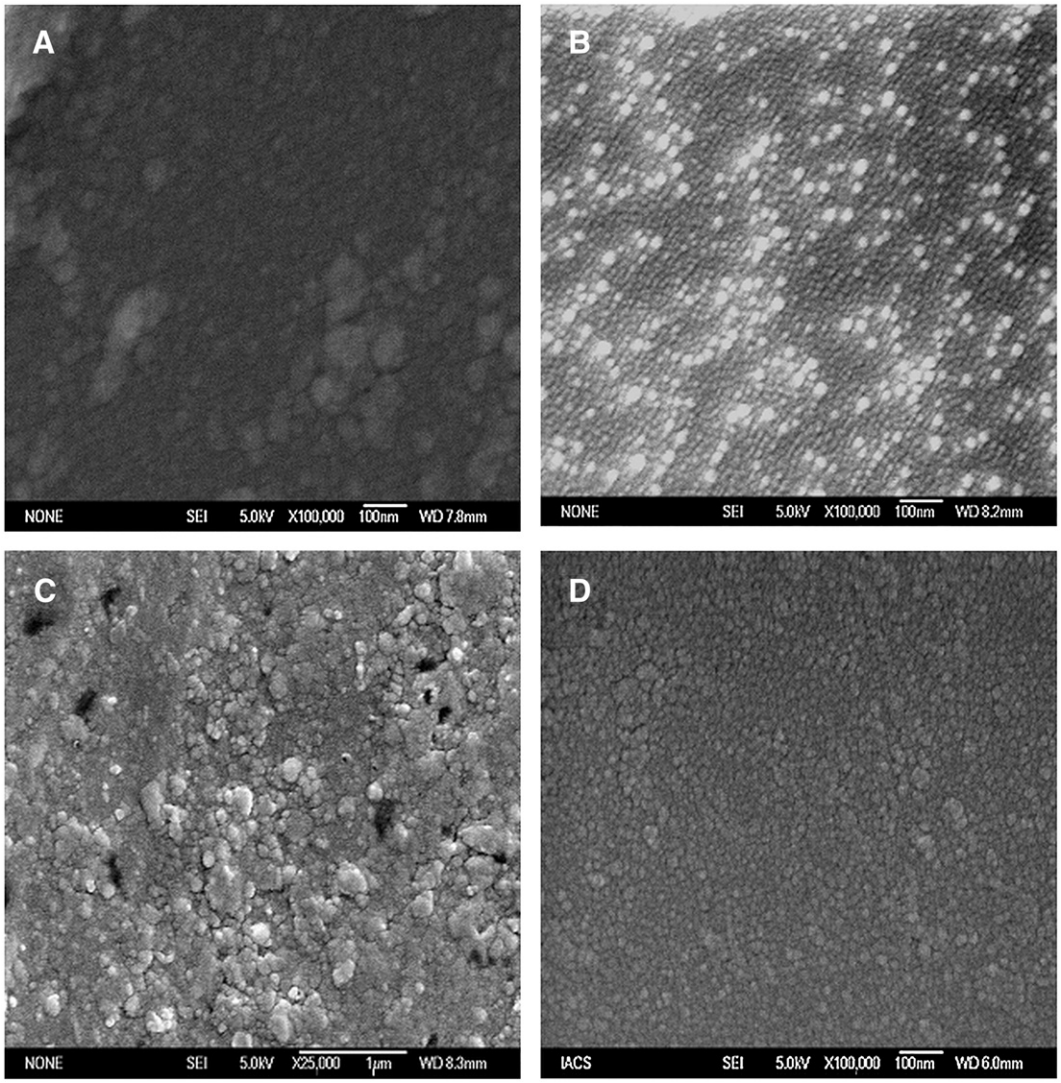

Fig. 7. FE-SEM images of transferred film. Panel A: pure ODA film. Panel B: PEP monolayer film transferred at $\pi = 35$ mN/m. Panels C and D represent the ODA–PEP LB film transferred at $\pi = 35$ and 20 mN/m, respectively from pure water subphase.

resolution. Surface is rough and the protein forms clusters and tend to amalgamate to form a layer of protein onto the ODA monolayer. This amalgamated layer consists of globular domain of PEP. Here, some patches (holes) are observed in the film in micrometer scale resolution. The overall results indicate that at very high surface pressure region, proteins are almost squeezed out from the ODA monolayer. Due to strong electrostatic interaction, some ODA expels into the subphase from film together with PEP and form holes. Some may squeezed out towards air creating protein rich upper layered structure. Therefore, the observation in isotherm is confirmed by FE-SEM imaging. Therefore, film should be transferred below the transition region ($\pi = 35$ mN/m) to avoid the squeezing out of PEP as well as for smooth film. To avoid the squeezing out of protein we transferred a film at 20 mN/m (Panel D), i.e., below the transition region. This film looks like a protein–lipid mixed film and composed of aggregates of ODA–PEP with dimension ranging from 20–50 nm in diameter.

4. Conclusion

We have studied the incorporation/entrapment of water-soluble surface-active enzyme pepsin (PEP) within an insoluble cationic octadecylamine (ODA) Langmuir monolayer. The observation suggests that the incorporation of PEP is less preferable at higher surface pressure. Natural bio membranes are in the pressure range ~30 mN/m. So we may say that PEP may not bind/penetrate to true biological membrane. The electrostatic interaction plays a significant role for the greater diffusion of PEP in cationic ODA monolayer. A double exponential association mechanism associated with diffusion and reorganization is responsible for the incorporation of PEP within ODA monolayer. The compressibility studies along with FE-SEM analysis indicate the squeezing out of PEP from the monolayer. It also helps us to select the optimum surface pressure to obtain a good quality and well-ordered Langmuir film. At high surface pressure region, protein is squeezed out from the surface. FE-SEM study also supports this observation. To get a good quality protein–lipid mixed film, the film should be lifted just below the transition region.

FTIR study of amide bands together with FE-SEM imaging of ODA–PEP mixed film indicate that ODA perturbs the PEP by the increment of β-structure resulting into larger unfolding, intra and intermolecular aggregates.

Acknowledgement

We thank DST, Government of India (Project No.: SR/S2/CMP-0051/2006) for partial financial support.

References

[1] A. Gole, C. Dash, M. Rao, M. Sastry, Chem. Commun. (2000) 297.
[2] A. Girard-Egrot, P.S. Godoy, L. Blum, J. Adv. Colloid Interface Sci. 116 (2005) 205.
[3] Y. Okahata, T. Tsuruta, K. Ijiro, K. Ariga, Langmuir 4 (1988) 1373.
[4] Y. Rui, S. Wang, P.S. Low, D.H. Thompson, J. Am. Chem. Soc. 120 (1998) 11213.
[5] L. Caseli, M.L. Moraes, V. Zucolotto, M. Ferreira, T.M. Nobre, M.E.D. Zaniquelli, U.P. Rodrigues Filho, O.N. Oliveira, Langmuir 22 (2006) 8501.
[6] A.G. Serrano, J. Perez-Gil, Chem. Phys. Lipids 141 (2006) 105.
[7] F. Beigi, P. Lundahl, J. Chromatogr. A 852 (1999) 313.
[8] J. Ramsden, J. Biosens. Bioelectron. 13 (1998) 593.
[9] J.B. Lee, D. Kim, J. Choi, K. Koo, Colloids Surf. B: Biointerfaces 41 (2005) 163.
[10] T. Kamilya, P. Pal, G.B. Talapatra, J. Phys. Chem. B 111 (2007) 1199.
[11] T. Kamilya, P. Pal, M. Mahato, G.B.J. Talapatra, Nanosci. Nanotechnol. 9 (2009) 2956.
[12] T. Kamilya, P. Pal, M. Mahato, G.B. Talapatra, Mater. Sci. Eng. C 29 (2009) 1480.
[13] K. Ariga, J.P. Hill, M.V. Lee, A. Vinu, R. Charvet, S. Acharya, Sci. Technol. Adv. Mater 9 (2008) 014109.
[14] P. Pal, D. Nandi, T.N. Misra, Thin Solid Films 239 (1994) 138.
[15] I. Hamachi, A. Fujita, T. Kunitke, J. Am. Chem. Soc. 116 (1994) 8811.
[16] V. Rosilio, M.M. Boissonnade, J. Zhang, L. Jiang, A. Baszkin, Langmuir 13 (1997) 4669.
[17] T. Kamilya, P. Pal, G.B. Talapatra, J. Colloid Interface Sci. 315 (2007) 464.
[18] F. Yin, A.K.M. Kafi, H. Shin, Y. Kwon, Thin Solid Films 488 (2005) 223.
[19] J.M. Chovelon, K. Wan, N. Jaffrezic-Renault, Langmuir 16 (2000) 6223.
[20] T. Kamilya, P. Pal, G.B. Talapatra, Colloids Surf. B: Biointerfaces 58 (2007) 137.
[21] P. Pal, T. Kamilya, M. Mahato, G.B. Talapatra, Colloids Surf. B: Biointerfaces 73 (2009) 122.
[22] C. Ybert, J.M. Di Meglio, Langmuir 14 (1998) 471.
[23] S.C. Biswas, L. Dubreil, D. Marion, J. Colloid Interface Sci. 244 (2001) 245.
[24] P.D. Boyer, H. Lardy, K. Myrback (Eds.), The Enzymes: Vol. 4, Academic Press, New York, 1960, ch. 4.
[25] L. Dubreil, V. Vie, S. Beaufils, D. Marion, A. Renault, Biophys. J. 85 (2003) 2650.
[26] J.S. Sharp, J.A. Forrest, R.A.L. Jones, Biochemistry 41 (2002) 15810.
[27] F. Yin, A.K.M. Kafi, H. Shin, Y. Kwon, Thin Solid Films 488 (2005) 223.
[28] E. Polverini, S. Arisi, P. Cavatorta, T. Berzina, L. Cristofolini, A. Fasano, P. Riccio, M.P. Fontana, Langmuir 19 (2003) 872.
[29] S. Korl, M. Ross, M. Sieber, S. Kunneke, H.J. Galla, A. Janshoff, Biophys. J. 79 (2000) 904.
[30] D. Lair, S. Alexandre, J.M. Valleton, Colloids Surf. B: Biointerfaces 45 (2005) 200.
[31] Lair, D. Ph. D. Thesis, University of Rouen, 1998.
[32] Z.W. Yu, J. Jin, Y. Cao, Langmuir 18 (2002) 4530.
[33] P. Ihalainen, J. Peltonen, Langmuir 19 (2003) 2226.
[34] F. Yin, H. Shin, Y. Kwon, Thin Solid Films 499 (2006) 1.
[35] J.B. Rosenholm, P. Ihalainen, J. Peltonen, Colloids Surf. A: Phys. Eng. Asp. 228 (2003) 119.
[36] P. Ihalainen, J. Peltonen, Sens. Actuators B 102 (2004) 207.
[37] M. Carbonaro, P. Maselli, P. Dore, A. Nucara, Food Chem. 108 (2008) 361.
[38] Protein –Ligand Interactions: structure and spectroscopy; A Practical Approach Edited by: S. E. Harding, B. Z. Chowdhry, Oxford University Press, Chapter 6 (2001).
[39] M. Jackson, H.H. Mantsch, Crit. Rev. Biochem. Mol. Biol. 30 (1995) 95.
[40] Selected applications of modern FT-IR techniques, K. Nishikida, E. Nishio, R. W. Hannah, Gordon and Breach publishers (Tokyo), 1995, pp. 268.
[41] T. Kamilya, P. Pal, M. Mahato, G.B. Talapatra, J. Phys. Chem. B 113 (2009) 5128.
[42] C. Bhattacharjee, S. Saha, A. Biswas, M. Kundu, L. Ghosh, K.P. Das, Protein Journal 24 (2005) 27.
[43] G.T. Meng, C.Y. Ma, Int. J. Biol. Macromol. 29 (2001) 287.
[44] Bandekar, J. Biochem. Biophys. Acta 1120 (1992) 123.
[45] K. Murayama, M. Tomida, Biochemistry 43 (2004) 11526.
[46] A. Barth, Biochim. Biophys. Acta 1767 (2007) 1073.
[47] M. Jackson, H.H. Mantsch, Can. J. Chem. 69 (1991) 1639.
[48] L. Sawer, C. Halt, J. Dairy Sci. 76 (1993) 3062.
[49] Y.L. Lee, Y.C. Yang, Y.J. Shen, J. Phys. Chem. B 109 (2005) 4662.